Communication

Infrared Brazing of $Ti_{50}Ni_{50}$ Shape Memory Alloy and 316L Stainless Steel with Two Sliver-Based Fillers

REN-KAE SHIUE, CHIA-PIN CHEN, and SHYI-KAAN WU

Dissimilar infrared brazing $Ti_{50}Ni_{50}$ and AISI 316L stainless steel using two silver-based fillers, Cusil-ABA and Ticusil, was evaluated. The shear strength of the Ticusil brazed joint is higher than that of the Cusil-ABA brazed one due to the formation of better fillet. The maximum shear strength of 237 MPa is obtained for the Ticusil joint brazed at 1223 K (950 °C) for 60 seconds. The presence of interfacial Ti-Fe-(Cu) layer is detrimental to the shear strength of all joints.

DOI: 10.1007/s11661-015-2830-7

$Ti_{50}Ni_{50}$ shape memory alloy (SMA) exhibits excellent shape memory effect, superelasticity, damping capacity, and corrosion resistance.[1,2] It has been applied in microactuator and micropump applications in micro-electro-mechanical systems.[3] The nominal composition of AISI 316L stainless steel (316L SS) is 0.03C, 12Ni, 17Cr, 2.5Mo, and balance Fe (wt pct).[4] 316L SS is covered by a protective oxide layer, causing it to have high oxidation and corrosion resistance in various environments. Both alloys are featured with excellent corrosion resistance, so joining of $Ti_{50}Ni_{50}$ and 316L SS shows potential for industrial application. However, there is one major problem in brazing $Ti_{50}Ni_{50}$ and 316L SS. The formation of brittle intermetallic compounds during brazing deteriorates the joint quality, especially at the interface between the braze alloy and substrate, and it has been reported in dissimilar brazing of the titanium alloy and stainless steel.[5,6]

The oxide films on 316L SS have been identified as multilayers mixed with iron-nickel oxide and chromium oxide.[4] Despite their excellent corrosion resistance, these oxide films have also proven to be a barrier to the wettability between 316L SS and general Ag-Cu filler metals.[7] Several studies revealed that the addition of Ti, an active ingredient, into Ag-Cu brazing alloys significantly improved the wettability while joining stainless steel or ceramic oxides.[8,9] Successful brazing of stainless steel or titanium alloys using Ag-based fillers was reported in previous studies.[10,11] Accordingly, Cusil-ABA (The Morgan Crucible Company, Berkshire, England) (Ag-35.25Cu-1.75Ti in wt pct) and Ticusil (The Morgan Crucible Company, Berkshire, England) (Ag-26.7Cu-4.5Ti in wt pct) braze alloys have been selected to braze $Ti_{50}Ni_{50}$ and 316L SS.

Infrared brazing is featured with a fast heating rate of up to 50 K/s, which is much higher than that of most traditional furnace brazing.[12] With the aid of accurate temperature control, it is highly suitable to evaluate the mechanism of early-stage reaction kinetics in brazing. Infrared brazing is applied in joining $Ti_{50}Ni_{50}$ and 316L SS using two active silver-based fillers. Microstructural evolution and shear strength of the brazed joints with various brazing conditions are assessed in the study.

Base metals used in the experiment were 316L SS and $Ti_{50}Ni_{50}$ SMA templates 15 mm in length, 7 mm in width, and 4 mm in thickness. The brazing surface was polished with SiC papers up to 1200 grit, and subsequently cleaned using an ultrasonic bath with acetone as the fluid prior to brazing. Both Cusil-ABA and Ticusil brazing foils were purchased from Wesgo Company (The Morgan Crucible Company, Berkshire, England), and the thickness of these brazing foils was 50 μm. The chemical compositions and melting behavior of the two brazing foils are listed in Table I.

The infrared furnace used in this study was a ULVAC SINKO-RIKO RHL-P610C (Ultra Clean Precision Technologies Corp., Tainan, Taiwan) with a maximum heating rate of 50 K/s. Infrared brazing was performed in a vacuum of 5×10^{-2} Pa, and the heating rate was set at 15 K/s throughout the experiment. All specimens were preheated at 973 K (700 °C) for 300 seconds prior to brazing in order to equilibrate the temperature profile of the specimen. Brazing conditions used in the experiment are summarized in Table II.

Shear tests were performed in order to evaluate the bonding strength of the brazed joint, and the tests were carried out on three specimens in each brazing condition. A symmetrical double lap joint, 316L SS/$Ti_{50}Ni_{50}$/316L SS, was proposed to perform shear testing of the brazed joint, as shown in previous studies.[12] Figure 1 illustrates the schematic diagram of the shear test sample.[12] The shear test specimen is enclosed in the graphite fixture with the shaded areas in the figure used in infrared brazing. Two bold black lines, 3.0-mm wide, in the middle of the graph indicate the brazing filler metal. Shear tests were conducted using a Shimadzu AG-10 universal testing machine (Shimadzu Corp., Nakagyo-ku, Japan) with a constant crosshead speed of 0.0167 mm/s. Cross sections of infrared brazed joints were cut by a low-speed diamond saw and subsequently examined using a NOVA 450 field emission scanning electron microscope (FESEM) (FEI Taiwan, Hsinchu, Taiwan) equipped with an energy-dispersive spectrometer (EDS). Its operation voltage was 15 kV, and the minimum spot size was 1 μm. X-ray structural analyses were carried out on selected fractured surfaces

REN-KAE SHIUE, Professor, is with the Department of Materials Science and Engineering, National Taiwan University, Taipei 106, Taiwan, ROC. CHIA-PIN CHEN, Graduate Student, is with the Department of Mechanical Engineering, National Taiwan University, Taipei 106, Taiwan, ROC. SHYI-KAAN WU, Professor, is with the Department of Materials Science and Engineering, National Taiwan University, and also with the Department of Mechanical Engineering, National Taiwan University. Contact e-mail: skw@ntu.edu.tw

Manuscript submitted October 21, 2014.
Article published online March 21, 2015

Table I. Chemical Compositions and Melting Temperatures of Two Brazing Foils

Braze Foil	Cusil-ABA	Ticusil
Chemical composition	63Ag-35.25Cu-1.75Ti (wt pct)	68.8Ag-26.7Cu-4.5Ti (wt pct)
Solidus temperature	1053 K (780 °C)	1103 K (830 °C)
Liquidus temperature	1088 K (815 °C)	1123 K (850 °C)

Table II. Summary of Infrared Brazing Conditions Used in the Experiment

Filler Foil	Brazing Temperature	Brazing Time (s)
Cusil-ABA	1143 K, 1173 K (870 °C, 900 °C)	300
Ticusil	1173 K, 1223 K (900 °C, 950 °C)	60, 180, 300

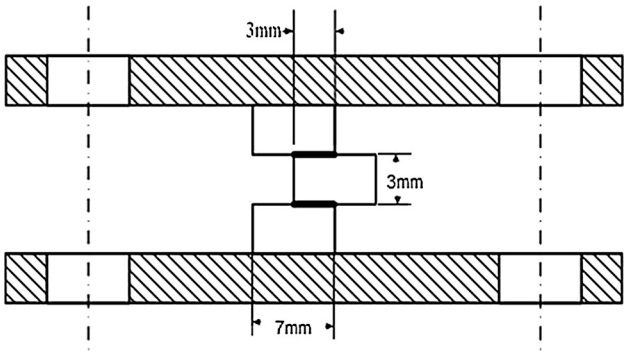

Fig. 1—Schematic diagram of the shear test specimen[12].

using a Rigaku TTRAX III high-power X-ray diffractometer (XRD). The Cu K_α was selected as the X-ray source. The X-ray scan rate was set at 0.0167 deg/s, and its range was between 35 and 80 deg.

Figure 2 shows the microstructural evolution of $Ti_{50}Ni_{50}$/Cusil-ABA/316L SS joints infrared brazed at various conditions. The white phase in the brazed zone is the Ag-rich matrix. Increasing the brazing temperature results in replacing the Ag-rich matrix by Cu-rich phase, as marked by G in Figure 2. A continuous intermetallic layer, as marked by A and B, is observed at the interface between $Ti_{50}Ni_{50}$ and the braze. According to the isothermal section of ternary Cu-Ni-Ti phase diagram at 1143 K (870 °C), the stoichiometry of this intermetallic layer shown in Figure 2 is close to the CuNiTi intermetallic compound.[13] The CuNiTi phase is a nonstoichiometric intermetallic compound, and it is also expressed as $(Cu_xNi_{1-x})_2Ti$, where x ranges from 0.23 to 0.75.[13] The EDS analysis results of A and B demonstrated in Figure 2 are consistent with the ternary Cu-Ni-Ti phase diagram.

There are at least two continuous reaction layers at the interface between the braze alloy and 316L SS substrate. One is the interfacial (Fe,Ni)Ti layer, marked by C and D, and the other is the interfacial Fe_2Ti layer, marked by E and F, as shown in Figure 2. Figure 3 illustrates the isothermal section of Cr-Fe-Ti at 823 K (550 °C) and the Cr_2Ti-Fe_2Ti pseudo-binary alloy phase

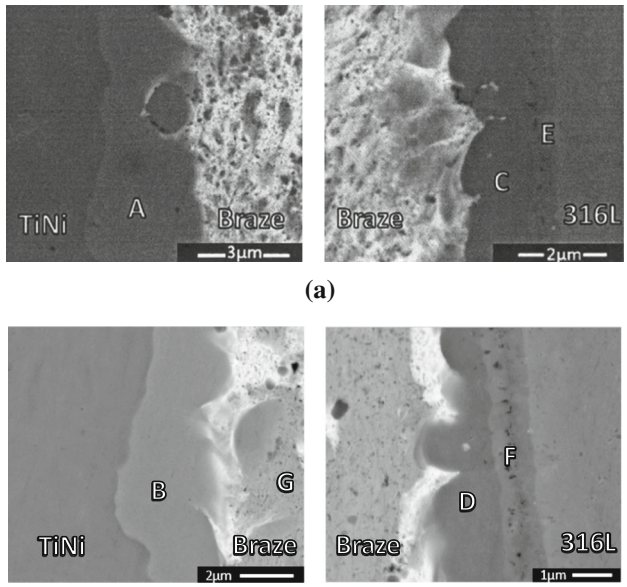

Element	A	B	C	D	E	F	G
Ti	31.9	29.9	46.1	45.5	35.1	32.8	---
Ni	28.2	26.7	14.2	16.2	4.0	4.6	---
Fe	---	---	25.0	24.9	44.5	50.4	---
Ag	---	---	---	---	---	---	6.6
Cu	39.9	43.3	12.9	12.1	3.4	---	93.4
Cr	---	---	1.8	1.4	13.0	12.2	---
phase	CuNiTi	CuNiTi	(Fe,Ni)Ti	(Fe,Ni)Ti	Fe_2Ti	Fe_2Ti	Cu-rich

Fig. 2—FESEM BEIs and EDS chemical analysis results in at. pct of $Ti_{50}Ni_{50}$/Cusil-ABA/316L SS joints infrared brazed at (*a*) 1143 K (870 °C) for 300 s and (*b*) 1173 K (900 °C) for 300 s.

diagrams.[13] Dissolution of $Ti_{50}Ni_{50}$ substrate into the molten braze results in high Ni and Ti contents in the melt. The Ti readily reacts with 316L SS during brazing and forms continuous Fe-Ti reaction layers. According

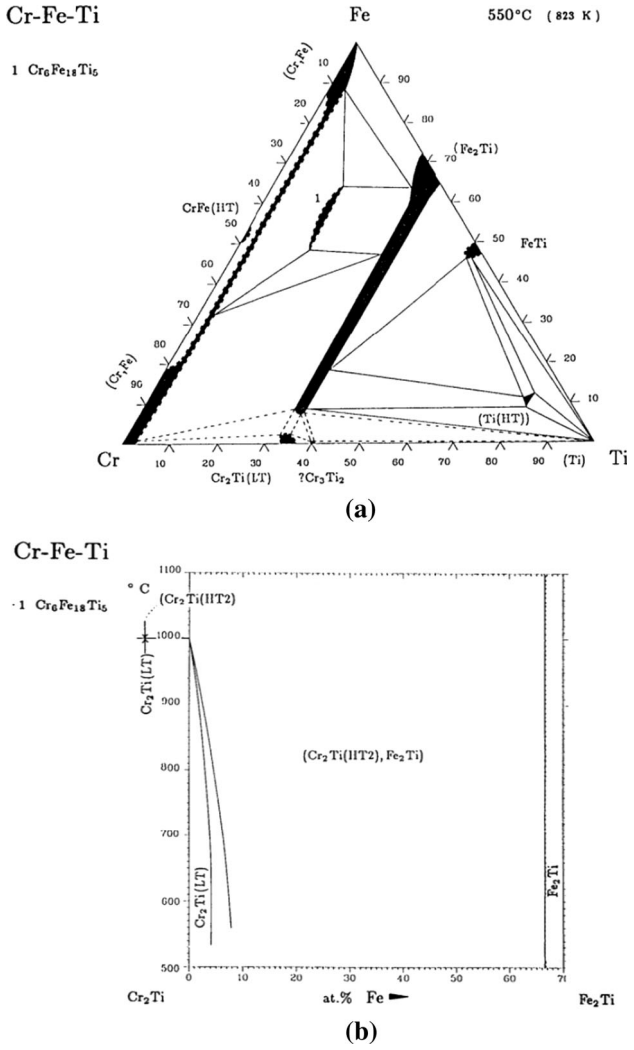

Fig. 3—Cr-Fe-Ti ternary alloy phase diagrams: (*a*) isothermal section at 823 K (550 °C) and (*b*) Cr_2Ti-Fe_2Ti pseudo-binary alloy phase diagram[13].

to Figure 3, Fe_2Ti dissolves a huge amount of Cr, and it is soluble with Cr_2Ti. A continuous FeTi intermetallic layer is also observed in the experiment. However, the solubility of Cr in FeTi intermetallic compound is much less than that in Fe_2Ti based on Figure 3(a). Limited Cr is dissolved in the FeTi phase, as demonstrated in C and D of Figure 2. Additionally, a huge amount of Ni is dissolved into FeTi compound and forms (Fe,Ni)Ti intermetallic phase based on the Fe-Ni-Ti ternary alloy phase diagram.[14] They are all consistent with the EDS chemical analysis results displayed in Figure 2. It is noted that increasing the brazing time has no significant influence on the thicknesses of these interfacial Ti-Fe intermetallic phases.

Figure 4 displays the microstructural evolution of $Ti_{50}Ni_{50}$/Ticusil/316L SS joints infrared brazed at 1173 K (900 °C) for various brazing time periods. The brazed area is primarily comprised of white Ag-rich matrix, Cu-rich phase, and many Cu-Ti intermetallics. The Ti content in Ticusil foil is higher than that in Cusil-ABA foil. It is expected that enhanced interfacial reaction among the braze melt and two substrates is observed. There is a continuous Cu_2Ti reaction layer, as marked by H and L, adjacent to the $Ti_{50}Ni_{50}$ substrate.[13] Additionally, Cu_3Ti_2 (marked by I, K, and M) is also observed from the brazed joint. The formation of these Cu-Ti intermetallic compounds is consistent with the Cu-Ti binary phase diagram.[14] In addition to Cu-Ti intermetallics, an interfacial Fe-Ti intermetallic compound is formed close to the 316L SS substrate. Tashi *et al*. showed that many silver-based fillers cannot act as barriers to prohibit the transport of Fe from 316L SS into braze, so brittle Fe-Ti or Cu-Fe-Ti intermetallics are formed.[6] Van Beek *et al*. suggested that TiCu can dissolve Fe up to 24 at. pct at 1123 K (850 °C) designated as $Ti_{0.43}Fe_xCu_{0.57-x}$, where x is between 0.21 and 0.24.[15] According to the EDS chemical analysis results, interfacial $Ti_{0.43}Fe_xCu_{0.57-x}$ phase, as marked by J and N in Figure 4, is observed.

Figure 5 shows the microstructural evolution of $Ti_{50}Ni_{50}$/Ticusil/316L SS joints infrared brazed at 1223 K (950 °C) for 60, 180, and 300 seconds. Enhanced interfacial reactions are caused by elevated brazing temperature. Ghosh *et al*. suggested that the brazing at higher temperature can widen the element diffusion zone and that it is easier to form intermetallics with more elements.[16] Based on this experimental observation, a higher brazing temperature or time results in enhanced dissolution of $Ti_{50}Ni_{50}$ substrate into the braze melt. With increasing the brazing time from 60 to 180 or 360 seconds, the interfacial Cu_2Ti, as marked by O, is replaced by CuNiTi, as marked by R and T, in Figure 5. Additionally, $Ti_{0.43}Fe_xCu_{0.57-x}$ compound is also observed at the interface between the braze and 316L SS, as marked by Q, S, and U in the figure. The experimental observation is consistent with that of Ghosh *et al*.[16]

Table III shows the average shear strengths of different joints with various brazing conditions. Shear strengths of joints using the Ticusil filler are higher than those using the Cusil-ABA one. The maximum shear strength of 237 MPa is obtained for the joint using the Ticusil filler infrared brazed at 1223 K (950 °C) for 60 seconds. Figures 6(a) and (b) display SEM backscattered electron image (BEI) cross sections and SEI fractographs after shear tests of brazed specimens with Cusil-ABA filler at 1173 K (900 °C) for 300 seconds and Ticusil filler at 1223 K (950 °C) for 60 seconds, respectively. According to Figure 6, joints with Cusil-ABA and Ticusil brazes are fractured at the interfacial $Ti_{0.43}Fe_xCu_{0.57-x}$ intermetallic layer adjacent to 316L SS substrate, as marked by arrows in the figure. Figures 7(a) and (b) show the XRD structural analysis results of fractured surfaces after shear tests of brazed specimens with Cusil-ABA filler at 1173 K (900 °C) for 300 seconds and Ticusil filler at 1223 K (950 °C) for 60 seconds, respectively. It is obvious that interfacial Ti-Fe-(Cu) intermetallic compounds dominate the fractured surface, consistent with the aforementioned results. All cracks are dominated by brittle fracture, and there is no distortion observed in the brazed area. The formation of the interfacial $Ti_{0.43}Fe_xCu_{0.57-x}$ reaction layer is detrimental to all brazed joints. Increasing the

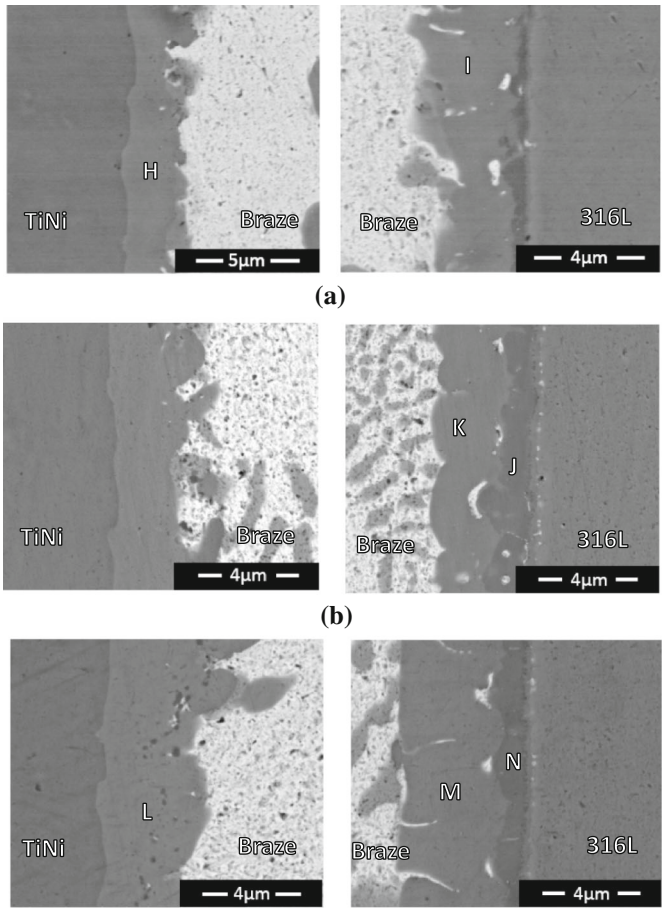

Element	H	I	J	K	L	M	N
Ti	31.2	37.8	44.9	37.6	30.0	39.9	46.5
Ni	8.7	3.2	5.5	5.9	4.6	2.6	4.3
Fe	---	8.9	27.8	7.5	---	7.6	25.0
Ag	1.6	1.5	---	1.1	2.5	4.4	---
Cu	58.5	48.9	18.3	47.9	62.9	45.6	22.1
Cr	---	---	3.5	---	---	---	2.1
phase	Cu_2Ti	Cu_3Ti_2	$Ti_{0.43}Fe_xCu_{0.57-x}$	Cu_3Ti_2	Cu_2Ti	Cu_3Ti_2	$Ti_{0.43}Fe_xCu_{0.57-x}$

Fig. 4—FESEM BEIs and EDS chemical analysis results in at. pct of $Ti_{50}Ni_{50}$/Ticusil/316L SS joints infrared brazed at 1173 K (900 °C) for (*a*) 60 s, (*b*) 180 s, and (*c*) 300 s.

brazing time results in the growth of interfacial $Ti_{0.43}Fe_xCu_{0.57-x}$ intermetallic compound, so lower shear strength is obtained from the $Ti_{50}Ni_{50}$/Ticusil/316L SS joint.

The wettability of the brazing filler melt to both substrates is quite different. Figures 8(a) and (b) illustrate fillets of $Ti_{50}Ni_{50}$/Cusil-ABA/316L SS and $Ti_{50}Ni_{50}$/Ticusil/316L SS joints, respectively. It is obvi-

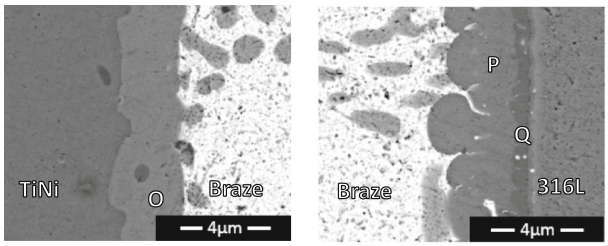

(a)

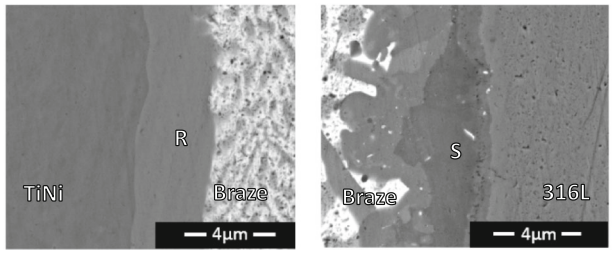

(b)

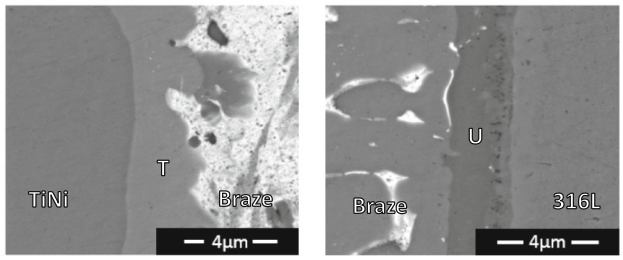

(c)

Element	O	P	Q	R	S	T	U
Ti	30.9	37.0	44.7	30.4	46.0	31.4	48.7
Ni	6.0	4.4	5.5	25.1	10.4	22.0	7.4
Fe	1.6	7.1	22.2	---	20.1	---	22.1
Ag	1.8	---	---	---	---	---	---
Cu	59.7	50.3	24.5	44.5	21.3	46.6	19.9
Cr	---	1.2	3.1	---	2.2	---	1.8
phase	Cu_2Ti	Cu_3Ti_2	$Ti_{0.43}Fe_xCu_{0.57-x}$	CuNiTi	$Ti_{0.43}Fe_xCu_{0.57-x}$	CuNiTi	$Ti_{0.43}Fe_xCu_{0.57-x}$

Fig. 5—FESEM BEIs and EDS chemical analysis results in at. pct of $Ti_{50}Ni_{50}$/Ticusil/316L SS joints infrared brazed at 1223 K (950 °C) for (*a*) 60 s, (*b*) 180 s, and (*c*) 300 s.

Table III. Average Shear Strengths of Infrared Brazed Joints

Brazing Foil	Brazing Temperature	Brazing Time (s)	Shear Strength (MPa)
Cusil-ABA	1143 K (870 °C)	300	66 ± 15
	1173 K (900 °C)	300	54 ± 27
Ticusil	1173 K (900 °C)	60	180 ± 7
	1173 K (900 °C)	180	99 ± 13
	1173 K (900 °C)	300	47 ± 19
	1223 K (950 °C)	60	237 ± 16
	1223 K (950 °C)	180	186 ± 20
	1223 K (950 °C)	300	88 ± 36

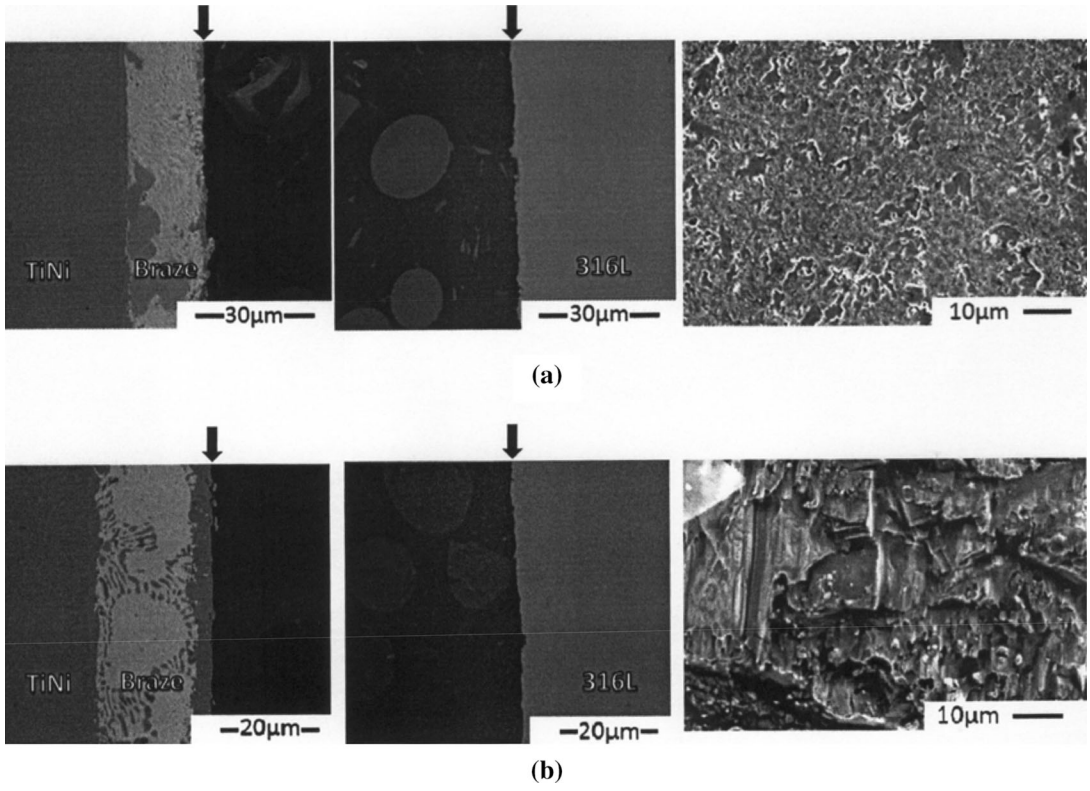

Fig. 6—FESEM BEI cross sections and SEI fractographs of (*a*) $Ti_{50}Ni_{50}$/Cusil-ABA/316L SS joint brazed at 1173 K (900 °C) for 300 s and (*b*) $Ti_{50}Ni_{50}$/Ticusil/316L SS joint brazed at 1223 K (950 °C) for 60 s after shear test.

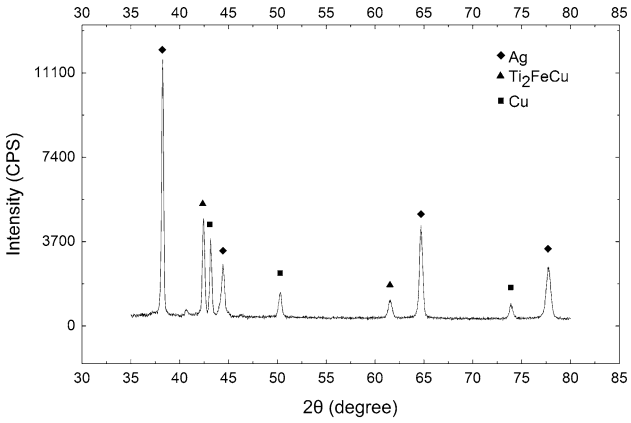

(a)

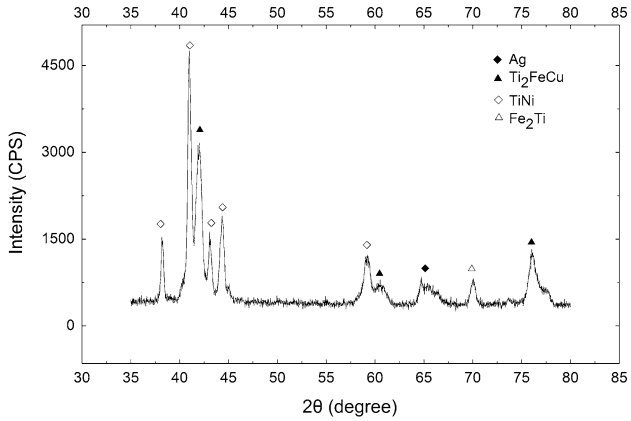

(b)

Fig. 7—XRD structural analysis of fractured surfaces after shear tests: (*a*) $Ti_{50}Ni_{50}$/Cusil-ABA/316L SS joint brazed at 1173 K (900 °C) for 300 s and (*b*) $Ti_{50}Ni_{50}$/Ticusil/316L SS joint brazed at 1223 K (950 °C) for 60 s.

ous that poor wetting of Cusil-ABA filler results in the formation of sharp fillet (Figure 8(a)). The presence of a sharp fillet suffers from stress concentration upon shear testing. In contrast, a fillet with smooth meniscus is formed using the Ticusil filler (Figure 8(b)). The smooth fillet provides extra contact area among the braze and two substrates, and the notch effect of stress concentration is avoided upon the shear test. Several studies have demonstrated the effect of fillet shape on the strength of brazed joint.[17,18] They are in accordance with the experimental results.

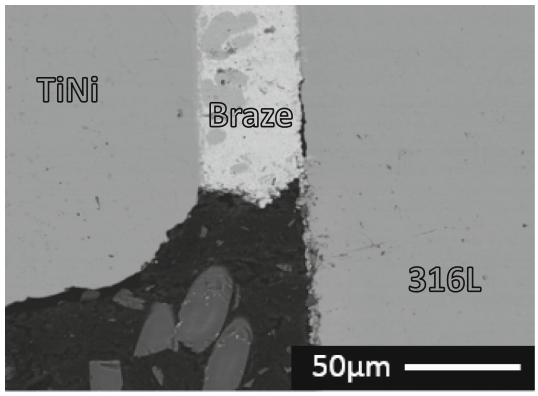

(a)

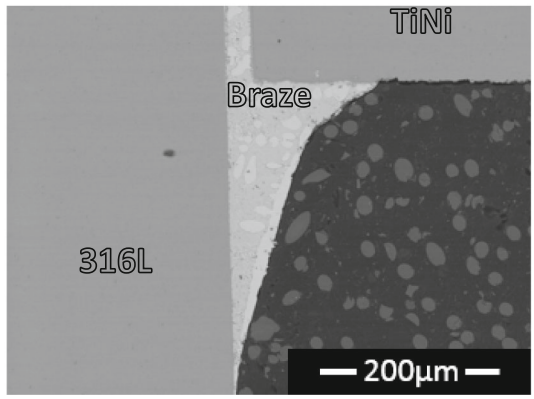

(b)

Fig. 8—FESEM BEI cross sections illustrating fillets of (*a*) $Ti_{50}Ni_{50}$/Cusil-ABA/316L SS joint at 1173 K (900 °C) for 300 s and (*b*) $Ti_{50}Ni_{50}$/Ticusil/316L SS joint at 1223 K (950 °C) for 180 s.

In summary, the brazed joint of $Ti_{50}Ni_{50}$/Cusil-ABA/316L SS is primarily comprised of Cu-rich phase and Ag-rich matrix. A continuous interfacial CuNiTi layer is observed close to the $Ti_{50}Ni_{50}$ substrate, and interfacial (Fe,Ni)Ti and Fe_2Ti reaction layers are formed close to the 316L SS side. The brazed joint of $Ti_{50}Ni_{50}$/Ticusil/316L SS is dominated by the Cu_3Ti_2 intermetallic phase and Ag-rich matrix. Continuous Cu_2Ti and CuNiTi reaction layers are formed at the Ticusil/$Ti_{50}Ni_{50}$ interface, and an interfacial $Ti_{0.43}Fe_xCu_{0.57-x}$ intermetallic layer is adjacent to 316L SS substrate. The maximum shear strength of 237 MPa is obtained for the Ticusil brazed joint at 1223 K (950 °C) for 60 seconds. The

difference in shear strengths is caused by wettability among the braze and two substrates and the presence of interfacial $Ti_{0.43}Fe_xCu_{0.57-x}$ reaction layer.

The authors gratefully acknowledge the financial support of this research by the Ministry of Science and Technology (MOST), Taiwan (Contract No. MOST 103-2221-E-002-063).

REFERENCES

1. K. Otsuka and K. Shimizu: *Int. Met. Rev.*, 1986, vol. 31, pp. 93–114.
2. K. Otsuka and X. Ren: *Progr. Mater. Sci.*, 2005, vol. 50, pp. 511–678.
3. Y. Fu, H. Du, W. Huang, S. Zhang, and M. Hu: *Sens. Actuator A*, 2004, vol. 112, pp. 395–408.
4. M.F. Montemor, M.G.S. Ferreira, N.E. Hakiki, and M. Da Cunha Belo: *Corr. Sci.*, 2000, vol. 42, pp. 1635–50.
5. J.G. Lee, S.J. Hong, M.K. Lee, and C.K. Rhee: *J. Nucl. Mater.*, 2009, vol. 395, pp. 145–49.
6. R.S. Tashi, S.A.A. Mousavi, and M.M. Atabaki: *Mater. Des.*, 2014, vol. 54, pp. 161–7.
7. O. Kozlova, R. Voytovych, M.F. Devismes, and N. Eustathopoulos: *Mater. Sci. Eng. A*, 2008, vol. 495, pp. 96–101.
8. A.P. Xian and Z.Y. Si: *J. Mater. Sci.*, 1990, vol. 25, pp. 4483–87.
9. X. Yue, P. He, J.C. Feng, J.H. Zhang, and F.Q. Zhu: *Mater. Charact.*, 2008, vol. 59, pp. 1721–27.
10. C.C. Liu, C.L. Ou, and R.K. Shiue: *J. Mater. Sci.*, 2002, vol. 37, pp. 2225–35.
11. R.H. Shiue and S.K. Wu: *Intermetallics*, 2006, vol. 14, pp. 630–8.
12. R.K. Shiue, Y.H. Chang, and S.K. Wu: *Metall. Mater. Trans. A*, 2013, vol. 44A, pp. 54–60.
13. P. Villars, A. Prince, and H. Okamoto: *Handbook of Ternary Alloy Phase Diagrams*, ASM International, Materials Park, OH, 1995.
14. T.B. Massalski: *Binary Alloy Phase Diagrams*, ASM International, Materials Park, OH, 1990.
15. J.A. van Beek, A.A. Kodentsov, and F.J.J. van Loo: *J. Alloys Compd.*, 1995, vol. 217, pp. 97–103.
16. M. Ghosh, S. Chatterjee, and B. Mishra: *Mater. Sci. Eng. A*, 2003, vol. 363, pp. 268–74.
17. H.L.J. Pang: *Int. J. Fatigue*, 1993, vol. 15, pp. 31–36.
18. Y. Verreman and B. Nie: *Fatigue Fract. Eng. Mater. Struct.*, 1996, vol. 19, pp. 669–81.